Title
Testing the N-Terminal Velcro Model of CooA Carbon Monoxide Activation.

Journal
Biochemistry, 57(21)

Authors
Tripathi, Sarvind
Poulos, Thomas

Publication Date
2018-05-29

DOI
10.1021/acs.biochem.8b00359

Peer reviewed

HHS Public Access

Author manuscript

Biochemistry. Author manuscript; available in PMC 2022 March 12.

Published in final edited form as:

Biochemistry. 2018 May 29; 57(21): 3059–3064. doi:10.1021/acs.biochem.8b00359.

Testing the N-Terminal Velcro Model of CooA Carbon Monoxide Activation

Sarvind Tripathi[†], **Thomas L. Poulos**[*]

Departments of Molecular Biology and Biochemistry, Pharmaceutical Sciences, and Chemistry, University of California, Irvine, Irvine, California 92697-3900, United States

Abstract

CooAs are dimeric bacterial CO-sensing transcription factors that activate a series of enzymes responsible for CO oxidation. The crystal structure of *Rhodospirillum rubrum* (rrCooA) shows that the N-terminal Pro from monomer A of the dimer coordinates the heme of monomer B that locks rrCooA in the "off" state. When CO binds, it is postulated that the Pro is replaced with CO, resulting in a very large reorientation of the DNA binding domains required for specific binding to DNA. Crystal structures of the closely related CooA from *Carboxydothermus hydrogenoformans* (chCooA) are available, and in one of these, the CO-bound on-state indicates that the N-terminal region that is displaced when CO binds provides contacts between the heme and DNA binding domains that hold the DNA binding domain in position for DNA binding. This has been termed the N-terminal velcro model of CooA activation. The study presented here tests this hypothesis by generating a disulfide mutant that covalently locks chCooA in the on-state. A simple fluorescence assay was used to measure DNA binding, and the S–S mutant was found to be in the on-state even without CO. We also determined the high-resolution crystal structure of the apo-heme domain, and the resulting structure is very similar to the holo-heme-bound structure. This result shows that the heme binding motif forms a stable structure without heme or the DNA binding domain.

Graphical Abstract

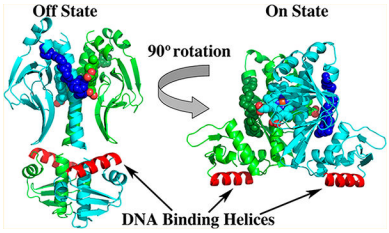

The CooA family of proteins consists of prokaryotic CO-sensing transcription factors that regulate the expression of genes involved in the utilization of CO as an energy source.[1] These are homodimeric proteins that contain two hemes. Each monomer has an N-terminal

[*]**Corresponding Author**: poulos@uci.edu. Phone: (949) 824-7020.

[†]**Present Address**: S.T.: Department of Chemistry and Biochemistry, University of California, Santa Cruz, Santa Cruz, CA 95064.

Accession Codes

Coordinates and structure factors have been deposited in the Protein Data Base as entry 6CPB.

The authors declare no competing financial interest.

heme binding domain and a C-terminal DNA binding domain. The binding of CO to the heme iron switches CooA to a state that binds to 5′ promoter sequences resulting in the transcription[2] of genes that enable CO to be utilized as an energy source.[3,4] The overall architecture of CooA closely resembles that of the catabolite activator protein (CAP) family of transcription factors that are regulated by cyclic AMP. The available crystal structures of CAP[5–7] are in the so-called on-state with the DNA domain in position to bind DNA. The crystal structure of *Rhodospirillum rubrum* (rrCooA)[8] was the first structure of a CAP-like transcription factor in the inactive off-state. A comparison of this off-state structure with the on-states of CAP shows that the DNA binding domain can undergo a very large reorientation between the on- and off-states. The off-state CooA crystal structure shows that the N-terminal Pro residue of monomer A coordinates the heme of monomer B and vice versa (Figure 1). In the presence of CO, the N-terminal Pro ligand is replaced by CO, resulting in a switch to the on-state. Crystal structures of a second CooA, *Carboxydothermus hydrogenoformans* CooA (chCooA), are available,[9,10] and one of these is in the CO-bound on-state. In this case, the N-terminal region is situated between the DNA and heme domains providing a series of nonbonded bridges between the two domains that has been postulated to hold the DNA domain in the active orientation. We have termed this the N-terminal velcro model of CooA activation (Figure 1).

Here we provide experiments designed to test this model. On the basis of the chCooA crystal structures, a mutant has been designed that should form an intramolecular S–S bond between the DNA and heme domains, thus locking chCooA in the on-state. In addition, a novel fluorescence assay has been developed that provides a simple and rapid method for differentiating between the on- and off-state conformations.

MATERIALS AND METHODS

FPLC-purified oligonucleotides were obtained from IDT. Restriction enzymes, T4 DNA ligase, and polymerase were purchased from New England Biolabs (Beverly, MA). Site-directed mutagenesis kits were purchased from Agilent Technologies. Ni-NTA agarose superflow resin and the miniprep plasmid purification kit were from Qiagen (Chatsworth, CA). Dithiothreitol (DTT), 5,5-dithiobis(2-nitrobenzoic acid) (DTNB), imidazole, hemin, and all other chemicals were purchased from Sigma-Aldrich and were of the highest quality. A Cary spectrophotometer (Agilent Technologies) was used for spectroscopic studies. A Hitachi F4500 fluorescence spectrophotometer was used for fluorescence studies.

Site-Directed Mutagenesis for Q4C and M177C.

On the basis of the crystal structure (Protein Data Bank entry 2HKX),[10] we designed a mutation to lock chCooA in the on-state. Amino acids Gln4 and Met177 were mutated to Cys by using standard site-directed mutagenesis and polymerase chain reaction. The Q4C/M177C double mutant is designated DMchCooA.

Expression and Purification of Wild Type chCOOA (WTchCOOA) and N127L/N128L and Q4C/M177C Mutants.

Wild type chCooA, double leucine mutants (N127L/S128L abbreviated as LLchCooA), and cysteine mutant proteins were purified by the same procedure reported previously by Clark et al.,[11] with a few modifications. Briefly, protein was overexpressed in *Escherichia coli* BL21(DE3) cells by induction with 1 mM IPTG at an OD of 0.6 and grown for a further 24 h at 25 °C; 0.4 μM δ-aminolevulinic acid was also added during induction for better heme incorporation. The IPTG-induced cells were harvested, resuspended in 50 mM Tris-HCl (pH 7.8), 500 mM NaCl, and 10 mM histidine (buffer A) and lysed by sonication. The crude lysate was centrifuged at 17000 rpm for 60 min. The supernatant was applied to a Ni^{2+}-NTA column pre-equilibrated with buffer A. Protein was eluted using the same buffer supplemented with 80 mM histidine. Fractions containing protein were pooled and concentrated by using a 10 kDa centricon. Concentrated protein was further purified and buffer exchanged by gel filtration using a Superdex 75 16/60 column equilibrated with 50 mM Tris (7.8) and 500 mM NaCl (buffer B). Protein fractions with a higher heme content (*R/Z*) were pooled and concentrated by using a 10 kDa cutoff centricon (Amicon). Protein concentrations were determined by using the extinction coefficient reported previously.[12] The purity of the protein was confirmed using 12% sodium dodecyl sulfate–polyacrylamide gel electrophoresis (SDS–PAGE).

Fe(II) and Fe(II)-CO samples were prepared anaerobically. The protein stocks were reduced with 50 mM dithionite in a nitrogen-filled anaerobic chamber, and extra dithionite was removed with a desalting column. For Fe(II)-CO, the Fe(II) CooA is exposed to CO in an anaerobic cuvette with a 1 cm path length.

Nonreducing PAGE and Determination of Free Thiol Groups by Ellman's Reagents.

Disulfide bond formation in the double-cysteine mutant was visualized by using nonreducing SDS–PAGE. Nonreducing gel electrophoresis was conducted using 12% polyacrylamide gels, and samples were loaded by mixing with dye without any reducing agent. Ellman's reagent[13] was used to quantitate free thiols; 500 μM Ellman's reagent [5,5-dithiobis(2-nitrobenzoic acid)] was incubated with 5 μM WTchCooA or double-cysteine mutants in 100 mM Tris (7.8), 300 mM NaCl, and 6 M guanidinium chloride for 15 min at room temperature. The absorbance is recorded by using a Cary 3E spectrophotometer at 412 nm, and the concentration of free thiol is calculated with a standard curve using cysteine. To calculate free thiol in proteins reduced by DTT, we used a desalting column (Bio-Rad) to remove excess DTT before recording spectra.

Fluorescence Spectrophotometer Studies for DNA Binding.

All fluorescence studies utilizing tyrosine emission were performed by using the synthetic oligonucleotide reported previously.[14] The sequence of half-sites contains a nucleotide derived from binding sites of one monomer of chCooA. Equimolar concentrations of the two strands were mixed to a final concentration of 1 μM in 50 mM Tris (7.8) and 100 mM NaCl. The strands were annealed by placing a solution at 90 °C and controlled cooling to 4 °C at a speed to 1 °C/min: ssDNA 1, 5′ GCGAAAAGTGTCAC; ssDNA 2, 5′ ATATGTGAC-ACTTTTC.

chCooA binds to DNA when the heme iron is reduced and bound to CO. To qualitatively analyze DNA binding, we used fluorescence spectroscopy to demonstrate binding of DNA to different states of native and DMchCooA at 25 °C on a Hitachi F4500 fluorescence spectrophotometer. chCooA does not have any tryptophan residue but does contain seven tyrosine residues that were used to monitor DNA binding. Proteins, oligonucleotide, and buffer were degassed and purged with argon to obtain the fluorescence data. Protein (3 μM) was excited at 272 nm, and emission spectra were recorded between 300 and 350 nm to monitor changes in fluorescence upon DNA binding in 50 mM Tris (pH 7.8), 300 mM NaCl, and 5 mM EDTA. Corrections were made by subtracting the spectrum of the appropriate buffer. The pUC19 plasmid is used as a control.

Cloning and Purification of the Heme Domain.

The heme domain (1–137) of chCooA was amplified via polymerase chain reaction from a plasmid containing chCooA and cloned between NcoI and XhoI with a C-terminal His tag in pET28a. Because the level of binding of heme to the heme domain is very low compared to that of the full length protein, 0.4 mM δ-aminolevulinic acid was also used during induction for better heme incorporation. The heme domain was purified by the same method used for purification of wild type and mutant full length protein except a low salt concentration (100 mM) was used during the final step of purification.

Heme Binding.

Heme binding was monitored by difference spectroscopy in the Soret region of the ultraviolet–visible spectrum at 25 °C. Successive aliquots of freshly prepared 1 mM hemin in 0.1 N NaOH were added to 7.5 μM heme domain and the reference cuvette. Difference spectra were recorded 5 min after the addition of each heme aliquot.

Crystallization, Data Collection, and Structure Solution of the Heme Domain.

The heme domain was crystallized by the hanging drop method, and the plates were incubated at 22 °C. Apo-heme domain crystals were obtained by mixing 2 μL of 400 μM protein and 1 μL of a reservoir solution containing 1.6–2.0 M ammonium sulfate and 100 mM Tris (8.5). Glycerol (30%) was used as a cryo-protectant, and a set of data were collected from a single crystal at SSRL beamline 7–1. Diffraction images were indexed, integrated, and scaled using Mosflm[15] and Aimless.[16]

The heme domain (2–143) of rrCooA[17] was used as a search model to determine the structure by molecular replacement calculations using Phaser[18] implemented in the CCP4 package.[19] The transformed model was subjected to refinement using Phenix.[20] Phases were improved and extended incrementally to 1.15 Å. The $2F_o - F_c$ and $F_o - F_c$ electron density maps were visualized, and model building was performed using COOT.[21] The crystallographic R_{factor} and R_{free} were monitored at each stage to avoid any bias. Water molecules were added by the automatic water-picking algorithm of COOT and inspected manually. The refined structure of the heme domain contains two chains and 301 water molecules. Final refinement statistics are listed in Table 1.

RESULTS AND DISCUSSION

Purification and Characterization.

The double-Cys mutant, DMchCooA, was overexpressed as a heme protein in the cytosolic fraction like WTchCooA and LLchCooA. Purified protein migrated as a single 26 kDa band via SDS–PAGE. Because imidazole acts as a proximal ligand to heme, we used histidine to elute proteins from the Ni-NTA column. The electronic absorption spectra of chCooA show Soret, α, and β bands at 421, 565, and 538 nm, respectively.

Mutant Design.

The structure of chCooA we reported[10] was that of a mutant called LLchCooA. Using an *in vivo* selection process, it was found that the conversion of Asn127 and Ser128 to Leu to give LLchCooA can enhance transcription in the absence of CO and hence must be locked in the on-state. As shown in Figure 2, Leu127 on helix F forms nonbonded contacts with Ala2 and Leu7. Comparing the rrCooA off-state and LLchCooA on-state structures shows that the DNA domain can reorient up to 180° (Figure 1). As shown in Figure 2, the DNA binding helix is oriented “down” in the on-state and thus is available for DNA binding, but in the off-state, this helix is oriented “up”. We have postulated that the reason the LLchCooA mutant adopts primarily the on-state conformation is that the mutant Leu127 side chain is exposed to solvent in the off-state but buried in the on-state where it can form favorable nonbonded contacts with Leu7 and Ala2. The N-terminal segment thus provides a series of nonbonded contacts between the DNA and heme domains that effectively holds the DNA domain in position for proper DNA binding. By displacing the N-terminal heme ligand, CO frees the N-terminal segment to form the link holding the DNA domain in the active orientation. The LLchCooA mutant shifts the equilibrium to the on-state even in the absence of CO because of the favorable burial of the mutant Leu127 side chain at the DNA–heme domain interface. To further test this view of CooA activation, we designed a mutant that will form an S–S bond between the heme and DNA domains, thus permanently locking chCooA in the on-state. Visual inspection of the LLchCooA structures indicates that mutating Met177 in the DNA domain and Gln4 in the heme domain should form an S–S bond when protein is in the on-state.

Disulfide Bond Formation.

To examine disulfide bond formation in the double mutant (DMchCooA), the purified protein was run on an SDS gel with or without a reducing agent (Figure 3). An intramolcular S–S bond generates a more compact structure that can potentially migrate toward lower molecular weights in SDS gels. WTchCooA runs as a single band with or without a reducing agent, while DMchCooA protein produces two bands under oxidizing conditions but only one band under reducing conditions. Treatment of DMchCooA with diamide, an oxidizing agent used to induce disulfide bond formation, increased the amount of the faster-migrating band. These results indicate the band migrating toward a lower molecular weight forms the intramolecular S–S bond.

The total numbers of free thiol groups in chCooA estimated from DTNB analysis under various treatments are listed in Table 2. These results show that there was only one free thiol

group per subunit of purified WTchCooA, while for DMchCooA, the number is greater than one. On the other hand, after treatment of chCooA and DMchCooA with DTT along with 6 M guanidinium chloride, the total thiol count is near three. Taken together, the SDS gels and thiol titration analysis indicate that a large fraction of DMchCooA forms an intramolecular S–S bond.

Binding of DNA to chCooA.

In seeking a relatively simple method for estimating DNA binding, we found that DNA induces strong quenching of the fluorescence of chCooA only when chCooA is in the CO complex. Because there is no tryptophan present in chCooA, we used a wavelength of 278 nm to excite tyrosine and recorded emission spectra over a range from 290 to 340 nm. As shown in Figure 4, WTchCooA binds to DNA only when the heme is reduced and bound to CO while Fe(II) DMchCooA in the absence of CO showed DNA binding.

Purification and Spectrophotometric Titration of the Heme Domain.

The purified heme domain behaves like wild type protein and Fe(II), formed by reducing the Fe(III) form with sodium dithionite, and showed Soret, α, and β bands at 424, 559, and 529 nm, respectively. Treatement of the reduced Fe(II) heme domain with CO revealed the spectral properties with Soret, α, and β bands at 421, 569, and 538 nm, respectively. Compared to the case for WTchCooA, when we purified the heme domain from E. coli it elutes with a very small amount of heme bound. We determined the stoichiometry of binding of heme to the heme domain to determine if the DNA binding domain plays a role in heme binding. Spectrophotometric titration of the heme domain of chCooA with a solution of hemin showed saturation at two hemes bound per dimer (Figure 5).

Heme Domain Structure.

We attempted to determine the structure of the chCooA heme domain dimer to determine if the N-terminus of molecule A coordinates the heme in molecule B, which is the case in rrCooA. Unfortunately, we were able to crystallize only the heme domain in the apo form without heme, although the heme domain contained a full complement of heme prior to setting up the crystallization drops (Figure 6). Even so, this ultra-high-resolution structure enables us to determine the influence of heme binding on the heme domain structure. A superposition of the heme domain monomer on the holo-chCooA monomer gives a root-mean-square deviation for Cα atoms of 1.6 Å, and most of the deviation is due to differences in surface loop regions. Thus, we can conclude that heme binding or the presence of the DNA binding domain has little influence on the structure of the heme domain. The one significant change relevant to heme binding is the position of the heme ligand, His82, in apo-chCooA. In one subunit of the dimer, His82 is oriented out toward the solvent away from the heme binding pocket. However, in the other monomer, His82 is oriented in and is in position to coordinate heme. Interestingly, the holo-chCooA structure has only one heme bound,[10] and in the monomer without heme, His82 also is oriented out toward the solvent.

CONCLUSIONS

The available CooA structures and the various structures of CAP provide a reasonably clear picture of the large motions involved in transcription factor activation. The DNA binding domains can reorient by 180° to place the DNA binding helices in the proper position for specific DNA interactions. The two domains are structurally independent given that the isolated heme domain crystal structures with or without heme are the same as in holo-CooA. CooA has provided some advantages over CAP in that a clearer picture has emerged on how the effector, in this case CO, triggers the required structural changes. The N-terminus of molecule A coordinates heme B and vise versa, thus locking the dimer in the off-state. The displacement of the N-terminus by CO frees the N-terminal peptide to provide a bridge between the heme and DNA binding domains. Hence, the N-terminal peptide serves as the “velcro” to hold the DNA domain in the orientation required for DNA binding. These changes also alter the heme binding pocket to favor binding of CO over that of other diatomic ligands, most notably O_2. Binding of oxygen to ferrous heme proteins is generally considered to favor ferric-superoxide, Fe(III)-OO^-, so H-bonding partners will help to stabilize the oxy complex. In CooA, the bound CO is surrounded by a Val and symmetry-related Leu residues along the dimer interface, thus creating a nonpolar pocket with no potential H-bonding partners.[10] This pocket is quite tight and favors a linear Fe–C–O angle rather than the bent angle preferred by O_2. The hydrophobic nature of the CO binding pocket and displacement of the Pro ligand are consistent with resonance Raman coupled with mutagenesis studies.[22,23] CooA thus provides a fascinating example of how diatomic sensing is coupled to large structural rearrangements of protein domains in addition to providing an example of how heme proteins can control ligand selectivity.

ACKNOWLEDGMENTS

This paper involves research performed at the Stanford Synchrotron Radiation Laboratory, a national user facility operated by Stanford University on behalf of the U.S. Department of Energy, Office of Basic Energy Sciences. The SSRL Structural Molecular Biology Program is supported by the Department of Energy, Office of Biological and Environmental Research, by the National Institutes of Health, National Center for Research Resources, Biomedical Technology Program, and by the National Institute of General Medical Sciences. The authors thank Prof. Gary Roberts for previous collaborations on CooA and the generous sharing of ideas and materials.

Funding

This work was supported by National Institutes of Health Grant GM57353 (T.L.P.).

REFERENCES

(1). Shelver D, Kerby RL, He Y, and Roberts GP (1995) Carbon monoxide-induced activation of gene expression in Rhodospirillum rubrum requires the product of cooA, a member of the cyclic AMP receptor protein family of transcriptional regulators. J. Bacteriol 177, 2157–2163. [PubMed: 7721706]

(2). He Y, Shelver D, Kerby RL, and Roberts GP (1996) Characterization of a CO-responsive transcriptional activator from Rhodospirillum rubrum. J. Biol. Chem 271, 120–123. [PubMed: 8550545]

(3). Ensign SA, Bonam D, and Ludden PW (1989) Nickel is required for the transfer of electrons from carbon monoxide to the iron-sulfur center(s) of carbon monoxide dehydrogenase from Rhodospirillum rubrum. Biochemistry 28, 4968–4973. [PubMed: 2504284]

(4). Kerby RL, Ludden PW, and Roberts GP (1995) Carbon monoxide-dependent growth of Rhodospirillum rubrum. J. Bacteriol 177, 2241–2244. [PubMed: 7721719]

(5). Passner JM, Schultz SC, and Steitz TA (2000) Modeling the cAMP-induced allosteric transition using the crystal structure of CAP-cAMP at 2.1 A resolution. J. Mol. Biol 304, 847–859. [PubMed: 11124031]

(6). Popovych N, Tzeng SR, Tonelli M, Ebright RH, and Kalodimos CG (2009) Structural basis for cAMP-mediated allosteric control of the catabolite activator protein. Proc. Natl. Acad. Sci. U. S. A 106, 6927–6932. [PubMed: 19359484]

(7). Schultz SC, Shields GC, and Steitz TA (1991) Crystal structure of a CAP-DNA complex: the DNA is bent by 90 degrees. Science 253, 1001–1007. [PubMed: 1653449]

(8). Lanzilotta WN, Schuller DJ, Thorsteinsson MV, Kerby RL, Roberts GP, and Poulos TL (2000) Structure of the CO sensing transcription activator CooA. Nat. Struct. Biol 7, 876–880. [PubMed: 11017196]

(9). Komori H, Inagaki S, Yoshioka S, Aono S, and Higuchi Y (2007) Crystal structure of CO-sensing transcription activator CooA bound to exogenous ligand imidazole. J. Mol. Biol 367, 864–871. [PubMed: 17292914]

(10). Borjigin M, Li H, Lanz ND, Kerby RL, Roberts GP, and Poulos TL (2007) Structure-based hypothesis on the activation of the CO-sensing transcription factor CooA. Acta Crystallogr., Sect. D: Biol. Crystallogr 63, 282–287. [PubMed: 17327664]

(11). Clark RW, Lanz ND, Lee AJ, Kerby RL, Roberts GP, and Burstyn JN (2006) Unexpected NO-dependent DNA binding by the CooA homolog from Carboxydothermus hydrogenoformans. Proc. Natl. Acad. Sci. U. S. A 103, 891–896. [PubMed: 16410360]

(12). Kerby RL, Youn H, Thorsteinsson MV, and Roberts GP (2003) Repositioning about the dimer interface of the transcription regulator CooA: a major signal transduction pathway between the effector and DNA-binding domains. J. Mol. Biol 325, 809–823. [PubMed: 12507482]

(13). Ellman GL (1958) A colorimetric method for determining low concentrations of mercaptans. Arch. Biochem. Biophys 74, 443–450. [PubMed: 13534673]

(14). Clark RW, Youn H, Parks RB, Cherney MM, Roberts GP, and Burstyn JN (2004) Investigation of the role of the N-terminal proline, the distal heme ligand in the CO sensor CooA. Biochemistry 43, 14149–14160. [PubMed: 15518565]

(15). Battye TG, Kontogiannis L, Johnson O, Powell HR, and Leslie AG (2011) iMOSFLM: a new graphical interface for diffraction-image processing with MOSFLM. Acta Crystallogr., Sect. D: Biol. Crystallogr 67, 271–281. [PubMed: 21460445]

(16). Evans PR, and Murshudov GN (2013) How good are my data and what is the resolution? Acta Crystallogr., Sect. D: Biol. Crystallogr 69, 1204–1214. [PubMed: 23793146]

(17). Kuchinskas M, Li H, Conrad M, Roberts G, and Poulos TL (2006) The role of the DNA-binding domains in CooA activation. Biochemistry 45, 7148–7153. [PubMed: 16752905]

(18). McCoy AJ, Grosse-Kunstleve RW, Adams PD, Winn MD, Storoni LC, and Read RJ (2007) Phaser crystallographic software. J. Appl. Crystallogr 40, 658–674. [PubMed: 19461840]

(19). Winn MD, Ballard CC, Cowtan KD, Dodson EJ, Emsley P, Evans PR, Keegan RM, Krissinel EB, Leslie AG, McCoy A, McNicholas SJ, Murshudov GN, Pannu NS, Potterton EA, Powell HR, Read RJ, Vagin A, and Wilson KS (2011) Overview of the CCP4 suite and current developments. Acta Crystallogr., Sect. D: Biol. Crystallogr 67, 235–242. [PubMed: 21460441]

(20). Adams PD, Afonine PV, Bunkoczi G, Chen VB, Davis IW, Echols N, Headd JJ, Hung L-W, Kapral GJ, Grosse-Kunstleve RW, McCoy AJ, Moriarty NW, Oeffner R, Read RJ, Richardson DC, Richardson JS, Terwilliger TC, and Zwart PH (2010) PHENIX: a comprehensive Python-based system for macromolecular structure solution. Acta Crystallogr., Sect. D: Biol. Crystallogr 66, 213–221. [PubMed: 20124702]

(21). Emsley P, and Cowtan K (2004) Coot: model-building tools for molecular graphics. Acta Crystallogr., Sect. D: Biol. Crystallogr 60, 2126–2132. [PubMed: 15572765]

(22). Coyle CM, Puranik M, Youn H, Nielsen SB, Williams RD, Kerby RL, Roberts GP, and Spiro TG (2003) Activation mechanism of the CO sensor CooA. Mutational and resonance Raman spectroscopic studies. J. Biol. Chem 278, 35384–35393. [PubMed: 12796503]

(23). Ibrahim M, Kerby RL, Puranik M, Wasbotten IH, Youn H, Roberts GP, and Spiro TG (2006) Heme displacement mechanism of CooA activation: mutational and Raman spectroscopic evidence. J. Biol. Chem 281, 29165–29173. [PubMed: 16873369]

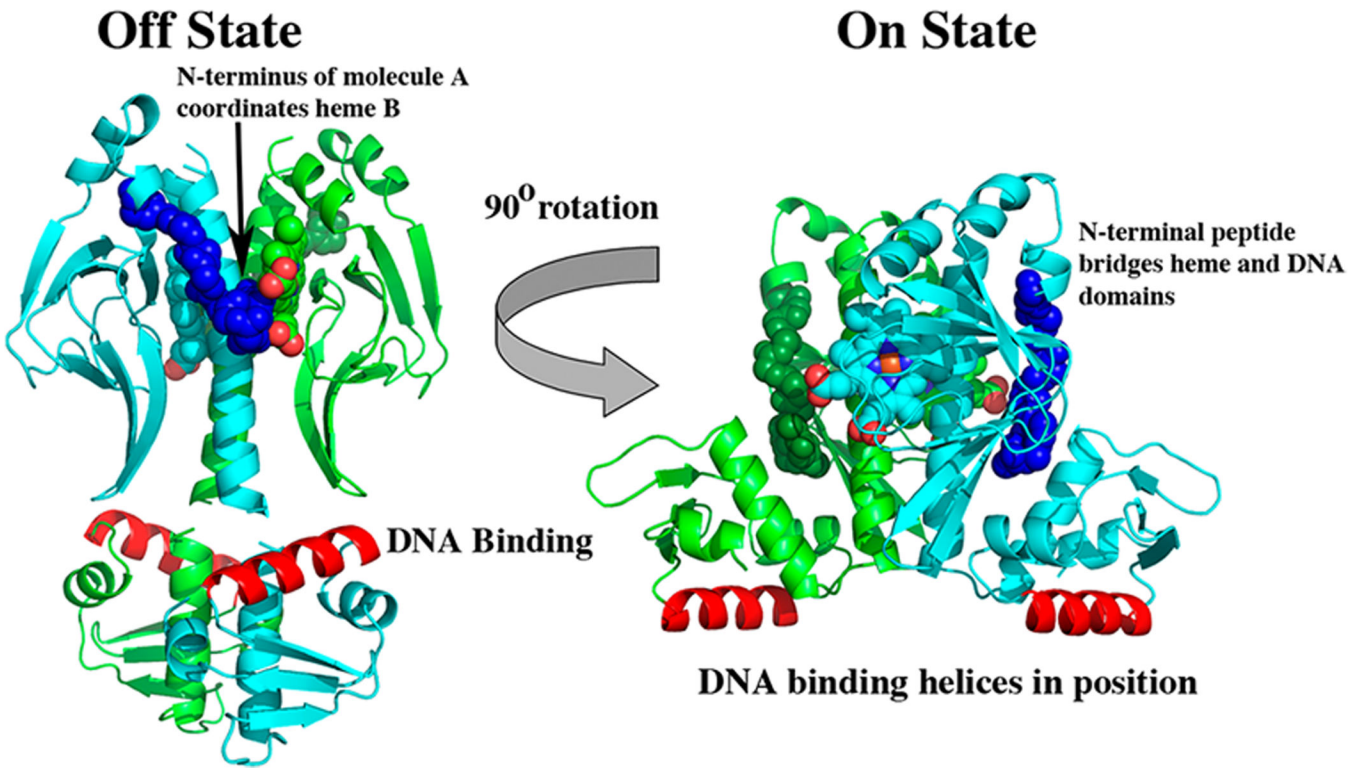

Figure 1.

Proposed on- and off-state structures of CooA. The model shown is a hybrid of the rrCooA off-state and chCooA on-state structures. In the off-state, the N-terminus of one molecule in the dimer (large dark blue and green spheres) coordinates the heme of the second molecule of the dimer. In the on-state, the N-terminal segment of molecule A serves as bridge between the heme and DNA binding domains that holds the DNA binding helices in an orientation suitable for DNA interactions.

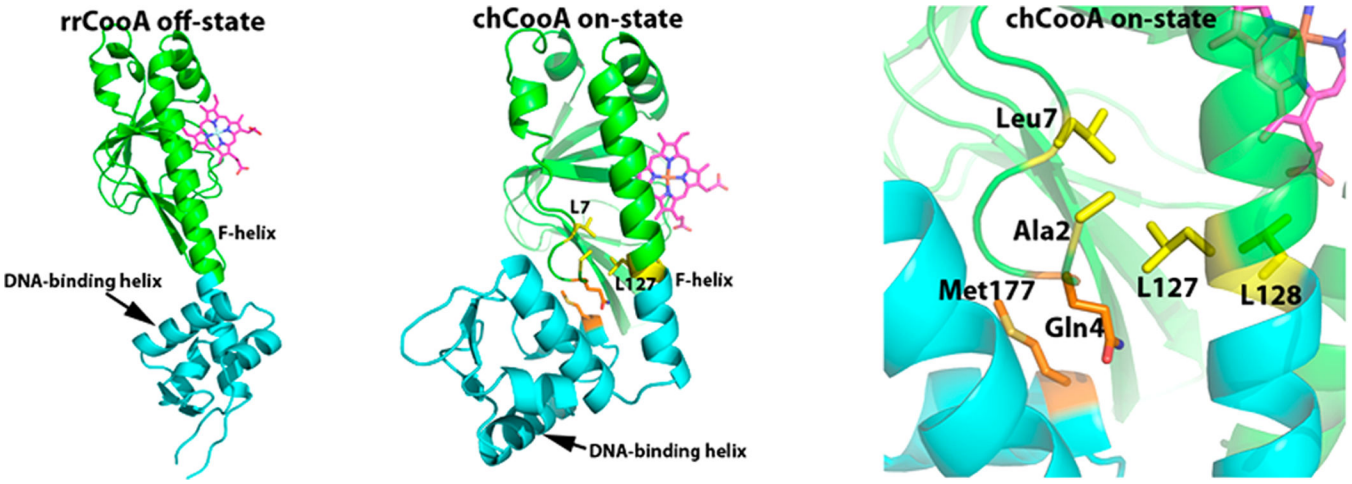

Figure 2.

Comparison of one monomer of off-state rrCooA and on-state chCooA. The N-terminal peptide of chCooA is situated between the DNA binding and heme domains. The Leu127 mutant side chain in the heme domain forms nonpolar interactions with Leu7 and Ala2. We hypothesize that these favorable interactions are one reason the N127L/S128L double mutant is locked in the on-state even in the absence of CO.

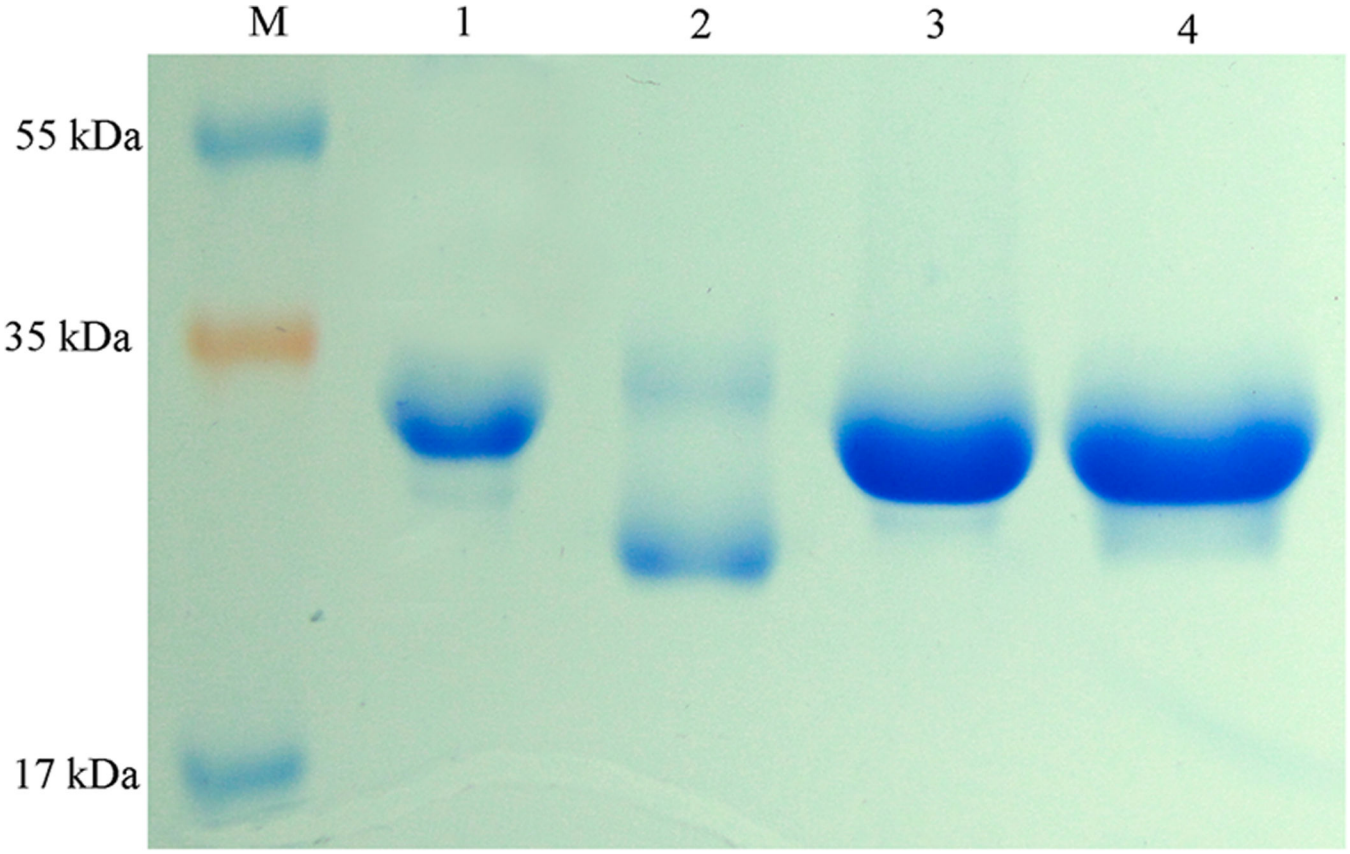

Figure 3.

SDS–PAGE of purified DMchCooA and WTchCooA. The purified protein is treated with or without a reducing agent in SDS loading dye and run on a 12% SDS–PAGE gel. Legend: lane M, molecular mass markers; lane 1, DMchCooA with a reducing agent; lane 2, DMchCooA without a reducing agent; lane 3, chCooA with a reducing agent; lane 4, chCooA without a reducing agent.

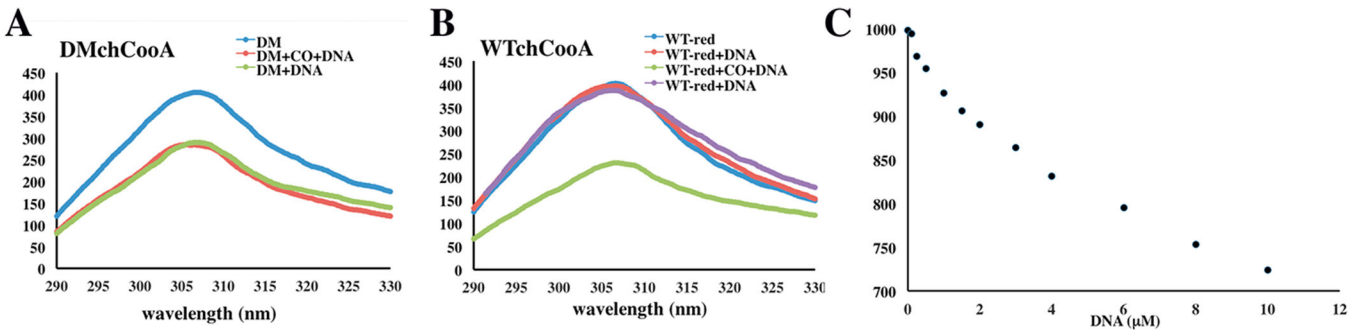

Figure 4.

Fluorescence emission spectra of WTchCooA and DMchCooA with DNA under anaerobic conditions. (A) Double mutant with an S–S bond. (B) WTchCooA. (C) DNA binding titration of 3 μM reduced DMchCooA in the absence of CO.

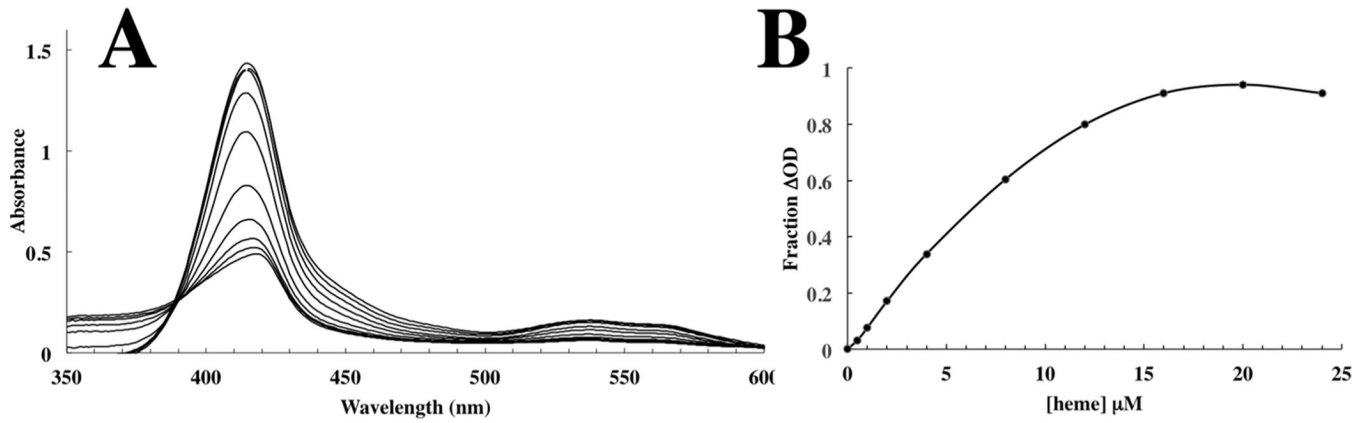

Figure 5.

Apo-heme domain (7.5 μM) titrated with increasing concentrations of heme. (A) Spectral changes with increasing heme concentration. (B) Fractional OD change as a function of heme concentration. Saturation is achieved at 1:1 heme:monomer ratio (two hemes per dimer).

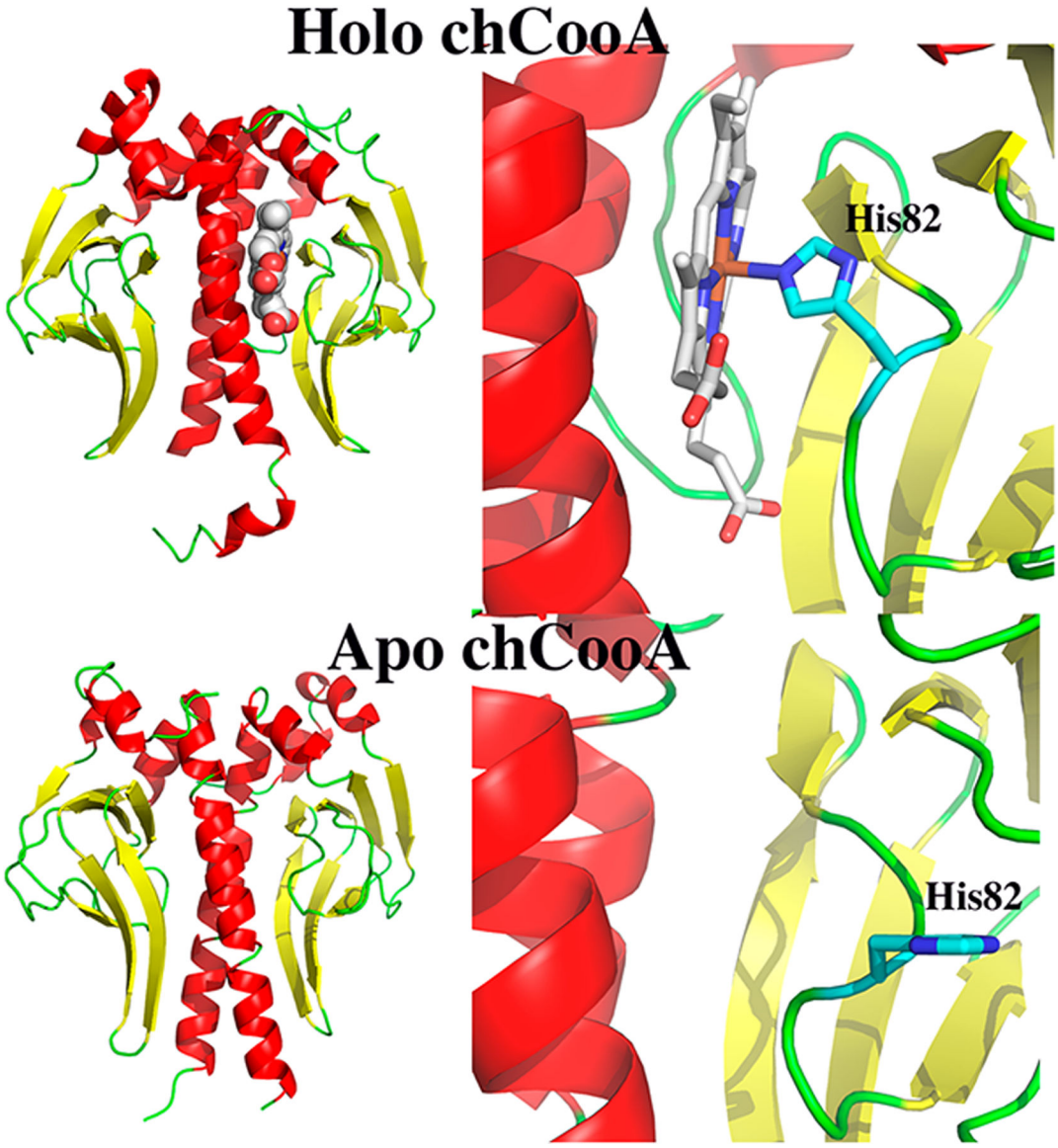

Figure 6.

Comparison of holo- and apo-chCooA heme domains. The overall dimeric structures are very similar, which shows that the heme domain folds in a manner independent of the heme cofactor or DNA binding domains. The one significant change in the active site is His82, which points out away from the heme pocket in one monomer of apo-chCooA.

Table 1.

Crystallographic Data Collection and Refinement Statistics

	Data Collection
space group	$P2_12_12_1$
unit cell dimensions	a = 64.66 Å, b = 65.82 Å, c = 72.88 Å, α = 90°, β = 90°, γ = 90°
resolution range (Å) (highest shell)	72.88–1.15 (1.17–1.15)
wavelength (Å)	1.127
total no. of observations	747009 (32152)
no. of unique reflections	109455 (5388)
R_{merge} [a]	5.0 (50.6)
$\langle I/\sigma \rangle$	14 (2.7)
$CC_{1/2}$	0.99 (0.89)
redundancy	6.8 (6.0)
completeness (%)	100 (99.2)
	Refinement
R_{work} (%)/R_{free} (%) [b]	13.0/14.9
no. of non-H atoms	2634
protein	2300
ligand/ion	33
water	301
B-factor (Wilson)	20
macromolecules	17.6
solvents	33.5
unmodeled residues	Ch. A, 1–6
	Ch. B, 1–7
root-mean-square deviation for bond lengths (Å)	0.007
root-mean-square deviation for bond angles (deg)	0.93
Ramachandran allowed/outliers (%)	100/0.0

[a] $R_{merge} = \sum_{hkl} \sum_i |I_{hkl} - \langle I_{hkl} \rangle| / \sum_{hkl} \sum_i (I_{hkl})$, where I_{hkl} is the intensity of an individual reflection and $\langle I_{hkl} \rangle$ is the average intensity over symmetry equivalents.

[b] $R_{work} = \| F_{obs}(h)| - |F_{calc}(h) \| / |F_{obs}(h)|$, where $F_{obs}(h)$ and $F_{calc}(h)$ are the observed and calculated structure factors, respectively. R_{free} is the R value obtained for a test set of reflections consisting of a randomly selected 5% subset of the data set excluded from refinement.

Table 2.

DTNB Titration of chCooA[a]

treatment	WTchCooA	DMchCooA
6 M GdmCl	0.7 ± 0.15	1.5 ± 0.2
6 M GdmCl and DTT	0.9 ± 0.12	2.8 ± 0.1

[a]Free thiol groups (RSH) per chCooA monomer (micromoles of RSH per micromole of subunit).